

Michael J. Yost, David Simpson, Kimberly Wrona, Stephen Ridley, Harry J. Ploehn, Thomas K. Borg and Louis Terracio
Am J Physiol Heart Circ Physiol 279:3124-3130, 2000.

You might find this additional information useful...

This article cites 23 articles, 12 of which you can access free at:

<http://ajpheart.physiology.org/cgi/content/full/279/6/H3124#BIBL>

This article has been cited by 2 other HighWire hosted articles:

Cyclical mechanical stretch modulates expression of collagen I and collagen III by PKC and tyrosine kinase in cardiac fibroblasts

B. Husse, W. Briest, L. Homagk, G. Isenberg and M. Gekle

Am J Physiol Regulatory Integrative Comp Physiol, November 1, 2007; 293 (5): R1898-R1907.

[Abstract] [Full Text] [PDF]

Integrins and the Myocardium

R. S. Ross and T. K. Borg

Circ. Res., June 8, 2001; 88 (11): 1112-1119.

[Abstract] [Full Text] [PDF]

Medline items on this article's topics can be found at <http://highwire.stanford.edu/lists/artbytopic.dtl> on the following topics:

Biochemistry .. Collagen

Engineering .. Shear Strain

Physiology .. Rats

Updated information and services including high-resolution figures, can be found at:

<http://ajpheart.physiology.org/cgi/content/full/279/6/H3124>

Additional material and information about *AJP - Heart and Circulatory Physiology* can be found at:

<http://www.the-aps.org/publications/ajpheart>

This information is current as of November 11, 2009 .

special communication

Design and construction of a uniaxial cell stretcher

MICHAEL J. YOST,^{1,2,3} DAVID SIMPSON,¹ KIMBERLY WRONA,¹ STEPHEN RIDLEY,¹
HARRY J. PLOEHN,³ THOMAS K. BORG,¹ AND LOUIS TERRACIO¹

¹Department of Developmental Biology and Anatomy and ²Department of Surgery,
University of South Carolina School of Medicine, and ³Department of Chemical Engineering,
University of South Carolina, Columbia, South Carolina 29208

Received 9 April 2000; accepted in final form 22 June 2000

Yost, Michael J., David Simpson, Kimberly Wrona, Stephen Ridley, Harry J. Ploehn, Thomas K. Borg, and Louis Terracio. Design and construction of a uniaxial cell stretcher. *Am J Physiol Heart Circ Physiol* 279: H3124–H3130, 2000.—In vitro mechanical cell stimulators are used for the study of the effect of mechanical stimulation on anchorage-dependent cells. We developed a new mechanical cell stimulator, which uses stepper motor technology and computer control to achieve a high degree of accuracy and repeatability. This device also uses high-performance plastic components that have been shown to be noncytotoxic, dimensionally stable, and resistant to chemical degradation from common culture laboratory chemicals. We show that treatment with glow discharge for 25 s at 20 mA is sufficient to modify the surface of the rubber to allow proper adhesion for polymerization of aligned collagen. We show through finite element analysis that the middle area of the membrane, away from the clamped ends, is predictable, homogeneous, and has negligible shear strain. To test the efficacy of the mechanical stretch, we examined the effect of mechanical stimulation on the production of β_1 -integrin by neonatal rat cardiac fibroblasts. Mechanical stimulation was tested in the range of 0–12% stretch and 0–10-cycles/min stretch frequency. The fibroblasts respond with an increase in β_1 -integrin at 3% stretch and a decrease at 6 and 12% stretch. Stretch frequency was found to not significantly effect the concentration of β_1 -integrin. These studies yield a new and improved mechanical cell stimulator and demonstrate that mechanical stimulation has an effect on the expression of β_1 -integrin.

mechanical cell stimulator; fibroblasts; integrins

IT IS WELL DOCUMENTED that cells and tissues in vivo are subjected to various forms of mechanical stimulation while performing their natural function (14, 28, 29). To study this phenomenon in a controlled environment, several types of in vitro mechanical cell stimulators have been developed (14, 24, 27). Most of these rely on

a flexible, resilient substrate coated with an extracellular matrix (ECM) material to which cells are attached. Attached cells are then processed through a controlled deformation regime. A variety of biological responses such as cell size, regulation, expression (10, 16, 20–22), synthesis (5–7, 12, 30), and degradation (7, 12, 23) of a variety of contractile and regulatory proteins are measured.

There are several uniaxial and equibiaxial cell stretchers available today in the literature and commercially. Biaxial stretchers allow the cells to be stretched along two axes perpendicular to each other without shear stress. The uniaxial stretchers allow cells to be stretched in one direction while experiencing compression in the perpendicular direction. The complication of shear stress in these systems can be minimized by careful design of the system and substrate geometry. There are distinct advantages to uniaxial cell stretch in approaching a number of biological problems. Previous devices have used a variable speed AC motor connected to an eccentric cam. The cam converts the rotational motion of the motor to a sinusoidal linear motion for the stretcher. The membrane containing the cells is submerged in a glass dish that also contains the culture medium. Two nylon clamps hold the membrane. One clamp is fixed, while the other is attached to the driven cam via a yoke and slide assembly. This type of device has yielded significant biological results but has not been particularly well engineered, primarily because the accuracy and reproducibility of the applied stress-strain have not been defined (4, 27).

The focus of this work was to apply engineering design principles and analysis to the design and construction of a new linear stretcher with greater accuracy and functionality. We then demonstrate the functionality of the stretcher by subjecting neonatal rat

Address for reprint requests and other correspondence: M. J. Yost, Dept. of Surgery and Developmental Biology and Anatomy, Univ. of South Carolina, School of Medicine, Columbia, SC 29208 (E-mail: Yost@med.sc.edu).

The costs of publication of this article were defrayed in part by the payment of page charges. The article must therefore be hereby marked “advertisement” in accordance with 18 U.S.C. Section 1734 solely to indicate this fact.

cardiac fibroblasts to well-defined stress-strain programs using the stretch system and measured the response of β_1 -integrin to various stretch conditions.

MATERIALS AND METHODS

Design of the cell stretcher. Figure 1 is a photograph of the cell stretcher assembly. The device applies a linear strain by displacing a 3-cm \times 6-cm rectangular membrane that is clamped along the short sides with the long sides left free. Two versions of the device have been built: a single and dual unit. The dual-stretch unit is the final design and will be the focus of this paper. Each device uses standard 150-mm culture dishes as the cell culture vessel.

The dual-stretch unit consists of a poly amide-imide base plate (Ultem 1000 DSM, Reading, PA) that fits inside a standard laboratory 150-mm culture dishes. The fixed end of the clamping mechanism is a press-fit poly-ether-etherketone (PEEK, DSM) rod assembly. The silicone rubber stretch membrane (0.01 in. thick, gloss finish; Specialty Manufacturing, Saginaw, MI) is attached using polytetrafluorethylene (PTFE) snap-on clamps. The displacement end of the clamping mechanism is a dual-rod slider mechanism constructed of PEEK. The membrane is clamped to one rod on the slider. A TiN (titanium nitride coating by Brycoat, Safety Harbor, FL)-coated stainless steel yoke assembly is attached to the other rod on the dual-rod slider. Motion is applied to the slider through the yoke assembly by a 0.1-in. per turn lead screw cartridge assembly (Deltron; Bethel, CT). A NEMA 23, 1.8° step, Hybrid Stepping motor (Pacific Scientific, Rockford, IL) is attached to the lead screw to supply the force to rotate the screw. The motor is controlled by a Pacific Scientific model 6445 hybrid stepping motor indexer and programmable controller (Pacific Scientific). The indexer is set to microstep at 1/125 step per pulse. The indexer uses a proximity switch to identify the mechanical home position (model IFRM 08N1504/L, Carolina Motion Control, Baumer Electric; Greenville, SC). The user interface is a Burr-Brown TM2500 OEM Microterminal (Carolina Motion Control, Baumer Electric, Greenville, SC) using RS232 communication protocol. The culture dish and lead screw are attached to an aluminum baseplate (type 2024-T351, Tull Metals; Columbia, SC) with a polycarbonate dust cover and can be installed in a suitable laboratory incubator. The motion profile is programmed into the controller with a laptop PC running PacSci Stepper Basic v3.0 (Pacific Scientific).

Two motion profiles are programmed: static and cyclic. For constant or static stretch, the user provides the required displacement. The stretcher goes to that displacement and

holds it there until the user ends the test, at which time the stretcher returns to the zero position. For cyclical stretch, the user provides the stretch displacement, frequency, and duration. After the set duration, the stretcher returns to the zero displacement position.

On power up, the unit finds the mechanical home position by adjusting the yoke position until it makes contact with the proximity switch. From this position, the user selects the desired motion profile using the OEM microterminal. The program prompts the user for specifics such as membrane size, desired percentage stretch, repeat frequency, and test duration. Candidate materials for use in the design of the stretcher culture dish insert were tested for cell toxicity and dimensional stability under autoclave and incubator conditions. The structural material candidates were PEEK, polycarbonate, HYDEX (polyester), Radel R (polyphenyl sulphone), Udel (polysulphone), Ultem 100 (polyetherimide) (DSM), and TiN-coated 316L stainless steel. All materials tested were found to be nontoxic to cells under our protocol. It was previously known that 316L stainless steel is toxic to cells. TiN-coated 316L stainless steel was found to be not toxic. The HYDEX material warped when subjected to the autoclave thus disqualifying it for use. None of the other candidate materials showed any sign of warping, swelling, or discoloration after testing.

Stretcher calibration. To determine the displacement of the stretcher yoke, we applied power to the unit and allowed it to find its mechanical home signal. We measured the inside dimension of the PEEK membrane holding rods using digital calipers (Brown & Sharp Manufacturing). We commanded the unit to move a distance of 5, 10, 15, and 20% stretch. After each move, the inside dimension was measured again and recorded. This procedure was repeated a minimum of three times. The distance traveled by each side of the slider while under load from the silicone membrane was measured to assess the deflection of each side of the cantilevered yolk assembly. The deflection was not detectable using digital calipers.

Membrane treatment. A rectangular membrane of 3 cm wide by 6 cm long by 0.025 cm thick was chosen to fit the stretch device used in the laboratory. For this project, we used the partial differential equations toolbox available for use with MatLab (13). We have shown using the plane stress module of the toolbox finite element analysis that the middle area of the membrane, away from the clamped ends, has predictable tension and compression, is homogeneous, and has negligible shear strain.

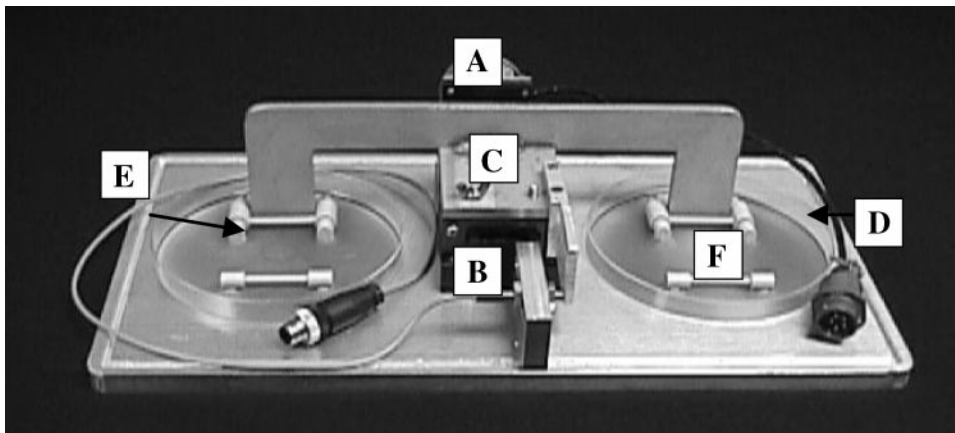


Fig. 1. Schematic of the cell stretcher. The components are as follows: A, stepping motor; B, lead screw; C, TiN-coated yoke; D, 150-mm culture dish; E, poly-ether-etherketone (PEEK) slider; and F, Ultem 1000 base plate. The stepping motor is driven from a programmable motor drive. The motion profile is entered into the drive via a microterminal interface (not shown). The cell stretch membrane is placed in between the PEEK slider components and clamped with polytetrafluorethylene (PTFE) clamps.

Although the clear silicone rubber membranes have many advantages, there has been little success getting extracellular matrix proteins such as collagen and especially aligned collagen gels (24) to polymerize and adhere to the rubber surface. We discovered that pretreatment with glow discharge sufficiently modifies the silicone polymer surface to allow aligned collagen gels to adhere and polymerize to the surface. Briefly, the polymer is made the anode for an electrical discharge over a potential of several thousand volts. The monomers (in this case residual monomer) can form a highly adherent, cross-linked film (19).

Pretreatment with glow discharge was found to be effective at enhancing the adhesion performance. Samples to be treated were placed in the treatment chamber of a standard SEM sputtercoating glow discharge unit (model E5100, Bio-Rad). The gold target was removed, and the unit was sealed as usual. Vacuum was applied to roughly 3×10^{-2} mbar of pressure. Dry argon was introduced into the chamber for 30 s at 1×10^{-1} mbar of pressure. Vacuum was restored to 3×10^{-2} mbar, and glow discharge was initiated. The applied voltage was roughly 2 kV. Treatment was tested at various amounts of time and at different current settings to determine the optimum.

Evaluation of adhesion performance. Adhesion of aligned collagen gels was evaluated by applying the collagen to the membrane using the methods of Simpson et al. (24). After the collagen was allowed to polymerize, the samples were inspected using a phase-contrast microscope and rated for adhesion (arbitrary ranking 1–5, with 1 being poor adhesion and alignment 5 being the best). The rating was done blinded to treatment condition. These data were evaluated using Excel (Microsoft, Redmond, WA) to determine the optimum conditions for best adhesion and best midpoint alignment. Figure 2 is a photomicrograph comparison of the 1, 3, and 5 rankings of collagen polymerization and adhesion. Figure 2A is *rank 1*, in which the collagen adhesion is extremely poor and the alignment is nonexistent. Figure 2B is *rank 3*; there are some gaps present in the coverage, and the fibers are not aligned parallel with the length of the membrane. Figure 2C is *rank 5*, where there is collagen polymerization and adhesion. The collagen coverage is complete and uniform. The collagen fibers are parallel to each other lengthwise on the membrane. It is important to note that, without pretreatment with glow discharge, the collagen coverage on the membranes is unsuitable for use as a cellular substrate.

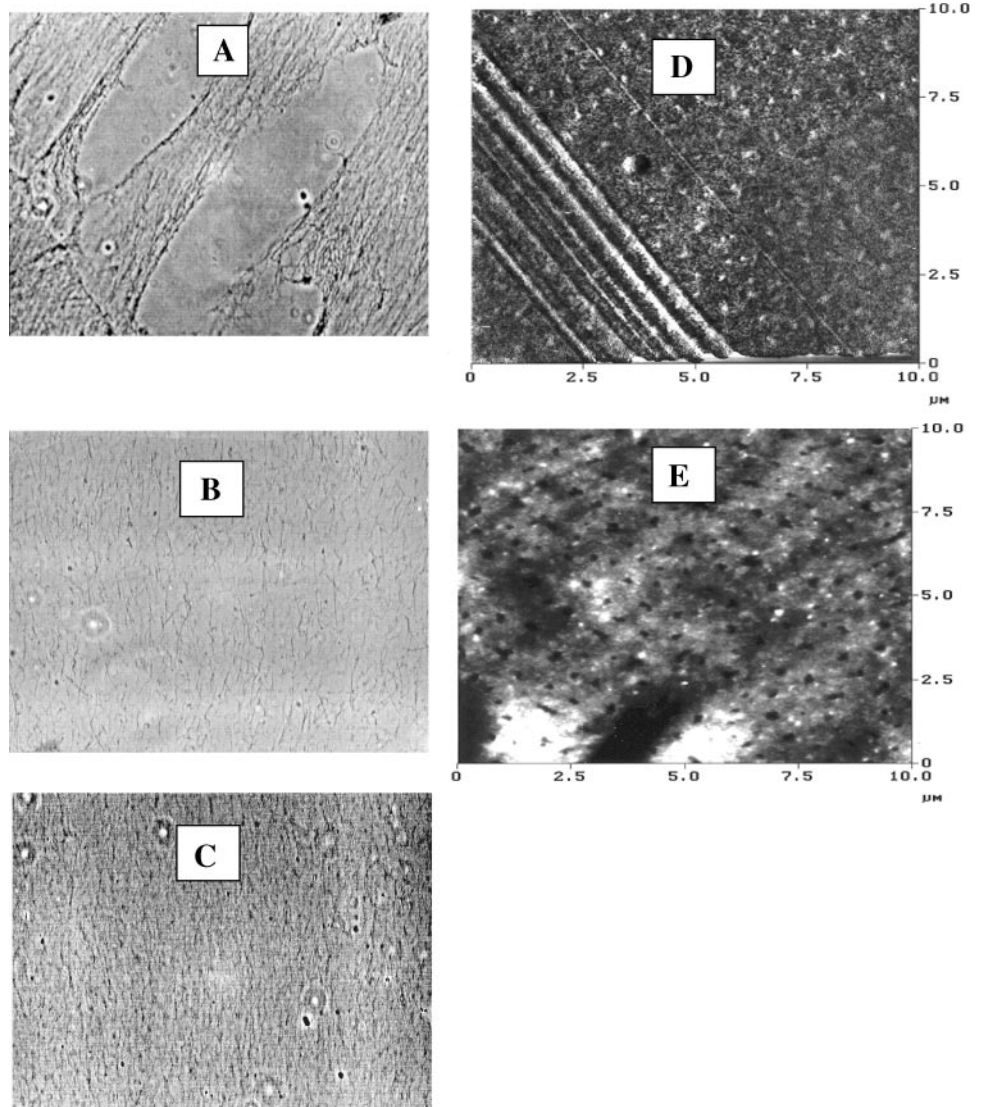


Fig. 2. A–C: photomicrograph comparison of aligned collagen on the silicone membrane. A: *rank 1*; B: *rank 3*; C: *rank 5* on the double-blind ranking scale. D and E: nanopores develop on the surface of the silicone membrane after treatment with glow discharge and can be detected by atomic force microscopy. Section analysis of the pores shows a radius of 625 nm and a depth of 7.29 nm. D: membrane before glow discharge treatment; E: after treatment at 20 mA for 15 s.

Atomic force microscopy. The surface of the silicone membranes was analyzed using atomic force microscopy and was performed before and after treatment; the results are shown in Fig. 2, *D* and *E*. Figure 2*D* is the membrane before glow discharge treatment and shows a relatively homogeneous surface with some surface debris and scratches but no pores. Figure 2*E* is after treatment at 20 mA for 15 s and shows a series of what appears to be nonrandom pores in the surface. Images were taken in tapping mode in air with uncoded Tapping Probe mode ("TESP") tips with a Digital Instrument Nanoscope MultiMode Scanning Probe Microscope (Santa Barbara, CA). The size of the pores was determined using the manufacturer's software. Section analysis of the pores shows a radius of 625 nm and a depth of 7.29 nm. The glow discharge created nanopores in the polymer film that may serve as anchorage points for the collagen fibrils.

Cell culture. All animals were housed in a facility approved by the American Association for Accreditation of Laboratory Animal Care, and protocols were approved by the Institutional Animal Care and Use Committee. Neonatal rat cardiac fibroblasts were isolated using the methods of Carver et al. (24). Silicone rubber stretch membrane (0.01 in. thick, gloss finish; Specialty Manufacturing) was prepared using glow discharge. They were subsequently coated with aligned collagen using the methods of Simpson et al. (24). Approximately 75,000 cells were plated on a 3-cm × 6-cm membrane by placing a cell-retaining ring, 2.36 cm ID and 2.7 cm OD, utilizing ~24% of the available area in the middle of the membrane and adding cells inside the ring. On the basis of the finite element model developed for these membranes, 67% of the area could be utilized with a retaining ring of the appropriate geometry. Cells were cultured in Dulbecco's modified Eagle's medium with 5% fetal bovine serum and 10% newborn bovine serum. The cells were allowed to attach for 24 h and then loaded in the stretcher apparatus to begin stretching. Stretch conditions were 3, 6, and 12% stretch at frequencies of 0 (static), 5, and 10 cycles/min. Cells were stretched for 12 h and then harvested at the end of the 12-h period. All stretch frequencies were continuous throughout the 12-h period. The experimental controls were cells plated on the aligned collagen-coated membranes but not stretched.

Integrin analysis. To determine the relative concentration of β_1 -integrin, the membranes were removed from the stretcher and rinsed three times with Moscona's saline, and the back of the membrane was blotted on a Kimwipe and transferred to a 100-mm culture dish. The cells were extracted with 150 μ l of RIPA buffer solution (in M: 0.15 NaCl, 0.015 NP-40, 0.012 deoxycholate, 0.003 SDS, and 0.5 Tris-base) and transferred to a cold room (4°C). Phenylmethylsulfonyl fluoride (20 μ l/ml) and benzamidine (10 μ l/ml) were added to the RIPA buffer and the cells scraped from the membrane. The solution and the cells were transferred to Eppendorf tubes and centrifuged at 14,000 rpm for 12 min. The supernatant was transferred to a new tube boiled for 10 min and stored at -20°C until analyzed. The pellet was discarded.

The β_1 -integrin was separated by gel electrophoresis on a 10% polyacrylamide gel. The loading of the gels was normalized on a per milligram of protein basis using a Pierce assay (Pierce, Rockford, IL) with a bovine serum assay (BSA) standard. The proteins were transferred to nitrocellulose for 1 h at 100 V with ice-pack stirring. The nitrocellulose blots were rinsed once in Tris-buffered saline (TBS)-Tween (T) (1 × TBS, 0.1% Tween 20) and blocked for 1.5 h in TBS-T containing 5% nonfat dry milk. The final concentration (2 μ g/ml) of rabbit anti- β_1 -integrin, prepared in our laboratory by the method reported in Xenophontos et al. (27), in 3% BSA and

phosphate-buffered saline was added and incubated overnight at 4°C overnight. The blots were rinsed three times (5 ml each) in TBS-T and then with rabbit horseradish peroxidase (Amersham, Piscataway, NJ) diluted 1:2,000 in blocking solution for 1.5 h. The blots were washed three times with TBS-T, developed using ECL reagents (Amersham, Piscataway, NJ), and exposed to film (Kodak Biomax, Eastman-Kodak, Rochester, NY). The exposed gel spots were analyzed with a spot densitometer (AlphaImager, Alpha Innotech, Oakland CA). Each experimental trial had a control, a static condition, and a cyclic condition (in duplicate). The data from each stretch trial were compared with the control sample for that trial and calculated as percent change from control. The data were then compared trial to trial on a percentage of control basis.

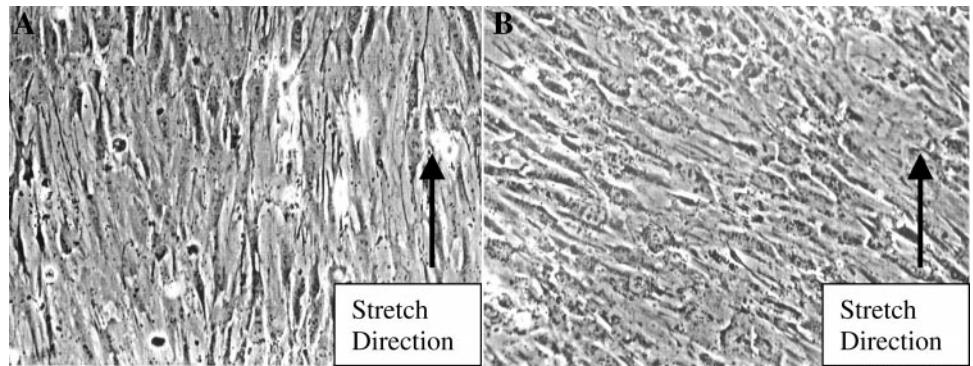
RESULTS

Stretcher calibration. During calibration, some of the overall capabilities of the stretcher were tested. This particular design is capable of a maximum strain of 24% for a 6-cm membrane. It also has a maximum linear speed of 72 cm/min, which translates into 20% strain at 30 cycles/min and 5% strain at 120 cycles/min on a 6-cm membrane. The linear displacement of the yoke was measured and found to be repeatable. The stretcher can be used on any anchorage-dependent cell type that will adhere to the silicone rubber substrate or an adherent coating on the substrate. Neonatal cardiac myocytes and fibroblasts were tested in this study. The finite element model developed for this project shows the strain on the silicone membrane will be proportional to the displacement of the yoke. This result verifies the accuracy of the displacement expected by the cell stretcher.

Cell culture. Figure 2*C* is a photomicrograph of aligned collagen attached to the silicone membrane before plating the cells. The stretch was parallel to the axis of collagen fibril orientation. We achieved good adhesion and stability of the collagen on the silicone. Figure 3 is a photomicrograph comparison of the fibroblasts on the aligned collagen gel before and after stretching. The cells aligned themselves with the collagen matrix during the attachment phase. The cells rotated to be more perpendicular to the direction of stretch during the stretch treatment. These results are consistent with what has been reported by previous investigators (27).

Integrin analysis. The Western blot analysis of the stretch experiments compared with controls are reported in Fig. 5 as percentage of control. Figure 4 shows representative Western blots for β_1 -integrin. In Fig. 4, lanes *A* and *B* are from a gel containing samples of 3% stretch and 5 cycles/min. Figure 4, lane *C*, is a control from this experiment. In Fig. 4, lanes *D*, *E*, *F*, and *G* are from another gel containing samples of 6% (*D* and *E*) and 12% (*F* and *G*) stretched at 10 and 5 cycles/min, respectively. Lanes *H* and *I* are from a control for this experiment. These bands show an increased intensity at 3% and decreased intensity at 6 and 12%. Figure 5 is the densitometric analysis of the Western blots for β_1 -integrin. Figure 5*A* is a comparison of all of the data points in the experimental set

Fig. 3. Fibroblasts attached to aligned collagen gels. *A*: fibroblasts attached to the aligned collagen gel before stretch. *B*: fibroblasts after stretching 3% at 5 cycles/min for 12 h. The rotation of the cells to align more perpendicular to the direction of stretch on the membrane is typical of the results seen in these studies.



versus the percentage stretch. The data are expressed as percentage of control. A linear regression of these data shows that the percent stretch is a significant factor in determining the concentration of β_1 -integrin with $P < 0.003$, $n = 60$. Figure 5B is a comparison of all of the data points versus the stretch frequency. A linear regression of these data shows that stretch frequency is not a significant factor determining the concentration of β_1 -integrin with $P < 0.72$, $n = 60$. Figure 5C is a comparison of the static stretch data versus percentage stretch. A linear regression of these data shows that static stretch alone is not a significant factor determining the concentration of β_1 -integrin with $P < 0.26$, $n = 20$. Figure 5D is a comparison of the cyclic stretch data versus percentage of stretch. A linear regression of these data shows that cyclic stretch was a significant factor determining the concentration of β_1 -integrin with $P < 0.006$, $n = 40$.

The overall result of these experiments is that at small deformations, 3%, the amount of β_1 -integrin increases with stretch and that at higher deformations, 6 and 12%, the amount of β_1 -integrin decreases. Cyclically stretching the cells gave a much stronger response than did static stretch, although the actual stretch frequency was not significant. The statically stretched cells showed the same trend as the cyclically stretched cells, but the magnitude of response was lower and not significant.

DISCUSSION

Stretcher design. It is well documented that cardiac cells are stretched in vivo while performing their natural functions in the heart (14, 27, 28). The objective of this study was to design and construct a uniaxial cell

stretcher and demonstrate its capabilities in a biological application. Although several uniaxial cell stretchers have been used successfully for biological experimentation, it was felt that a well-designed, accurate, and repeatable apparatus would be very useful in further investigations in the field. The design uses a disposable plastic cell culture dish with a reusable plastic baseplate insert. The design is based on the uniaxial cell stretcher developed and used by Simpson et al. (24) and the cyclical stretcher developed and used by Terracio et al. (28). High-performance plastic materials were required to survive and maintain dimensional stability through all of the commonly used processes for sterilization and incubation. Materials not only had to withstand the autoclave and incubator temperatures, they also had to be chemically resistant to the cell culture media and 70% ethanol commonly used as a localized sterilization technique. The materials selected also had to be ultraviolet (UV) stable to survive UV treatment common in some sterilization procedures. All of the materials tested were found to be noncytotoxic. This made the selection process criteria one of cost, availability, chemical resistivity, and structural suitability rather than toxicity. Although in the original prototypes, polysulphone was selected as the base-plate material, it was later found, during production, to be too brittle for the specified press fit of the PEEK components. Several new material candidates were tried, and the Ultem 100 (polyetherimide) was found to be superior and was selected.

Cell culture. After the 3% stretch treatment, the cells have realigned themselves to be roughly 70° off the primary stretch axis. This phenomenon is similar to previous observations where fibroblasts aligned per-

Fig. 4. Representative blots from the Western analysis of the β_1 -integrin from the various experiments. *Lanes A and B* are from a gel containing 3% stretch and 5 cycles/min samples. *Lane C* is a control from this experiment. *Lanes D–G* are from another gel containing 6% (*lanes D and E*) and 12% (*lanes F and G*) stretch at 10 and 5 cycles, respectively. *Lanes H and I* are from a control for this experiment.



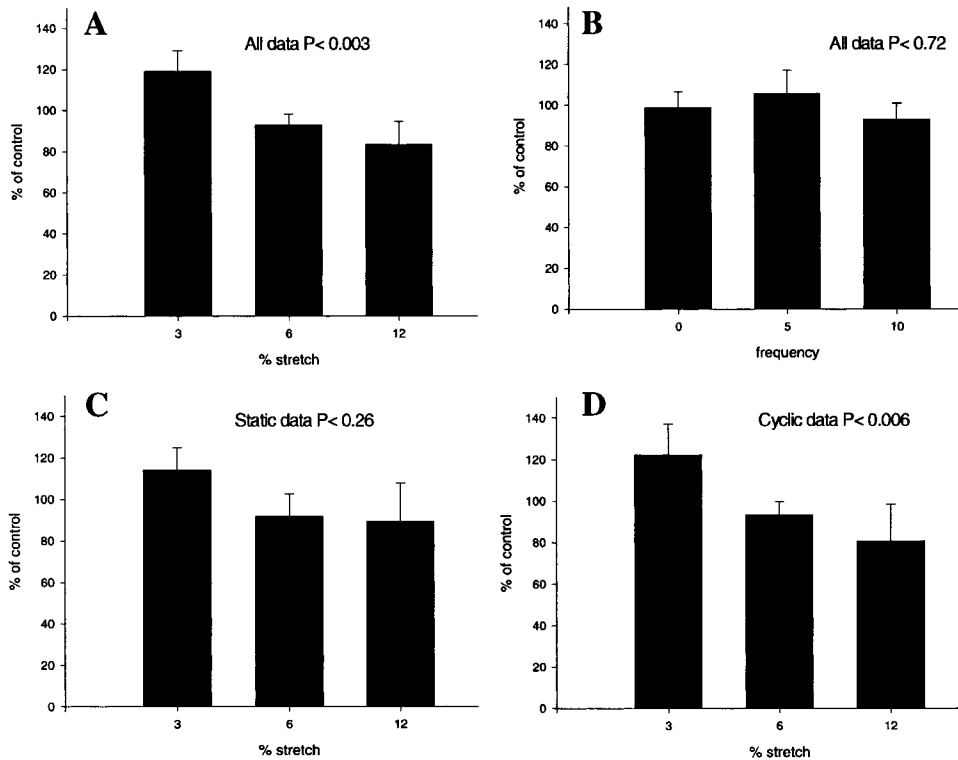


Fig. 5. Comparison of the β_1 -integrin response data to the various stretch conditions. *A*: all of the data plotted against percentage of stretch. *B*: all of the data plotted against stretch frequency. *C*: static stretch data plotted against percentage of stretch. *D*: cyclic stretch data plotted against percentage of stretch. These panels show that the percentage of stretch is significant to the concentration of β_1 . The response to percentage of stretch for cyclic stretch was greater than for static stretch, and stretch frequency had no impact on β_1 -integrin in the range of 5–10 cycles/min.

pendicular to the direction of stretch after 48–72 h of cyclic stretch (27). It has been proposed that the cells are responding to an off-axis force vector as a result of uniaxially stretching the rubber substrate (shear stress) (26). This hypothesis is inconsistent with the plane stress analysis completed by the author. In that analysis, there is no force or deformation vector present to cause the cells to rotate. In the stretch membrane area of interest, there is only compression and tension that are perpendicular to each other. The shear stress present is negligible in the area of the membrane of interest. Shear stress appears most significantly near the clamped edges of the membrane. The rotation of the cells is possibly caused by the interaction of the cell with the collagen α -helix twisting and untwisting in response to the stretch than by the rubber substrate deformation.

Integrin analysis. Integrins are transmembrane proteins that serve as an interface between the cellular cytoskeleton complex and the extracellular matrix (3). Integrins play a vital role in the transduction of mechanical information from the ECM to the cell nucleus via the cytoskeleton complex (3). Integrins have two components, a variable α -chain and an invariant β -chain. β_1 -Integrin, as well as many associated α -integrins, serve as mechanical signal transducers for the cell and are essential in the morphogenic process associated with heart development (1) and play an important role in the cellular development process. Given the critical mechanical communications role of β_1 -integrin, it was a good candidate to test the efficacy of the new cell stretcher. There was a definite response of β_1 -integrin to stretch. The increase of β_1 -integrin at low

deformations and the subsequent decrease at higher deformations was not originally predicted. It was predicted that the β_1 -integrin would increase with increasing percentage of stretch as the cell attempts to hold on to the substrate. It could be speculated that at the low deformations the cells are producing more integrin to improve the anchorage stability. At high deformations, the cells are cleaving off integrins and are attempting to adapt the new environment.

The lack of response to stretch frequency and the intensified response to percentage stretch of cyclically stretched cells was not predicted. However, a possible explanation is that the response is similar to that of the body to exercise. Repeated exercise (cyclic stretch) should result in a greater response than that to a single event (static stretch).

Linear regression analysis was sufficient to determine that percentage stretch had a significant impact on β_1 -integrin concentration. It also showed that although the percentage of stretch was important, there are likely other factors influencing the concentration of β_1 -integrin. The R^2 statistic for these experiments never exceeded 0.5, suggesting that other factors also have a significant impact on the concentration of β_1 -integrin.

In vivo, heart muscle is routinely stretched by up to 20% at frequencies of 150 cycles/min. However, these data would suggest that there would be a substantial downregulation of β_1 -integrin at these conditions. One can only speculate that the in vivo conditions are sufficiently different from the in vitro conditions used here that no exact correlation can be drawn between the degree and rate of stretch in the two conditions. How-

ever, in vitro experiments should provide insight into the in vivo situation, even though the magnitude and frequency are different.

These studies have produced an accurate and repeatable stretcher device. The device was demonstrated in a biological application to yield repeatable results. This device should prove very useful for biological investigations of the effect of mechanical stimulation on anchorage-dependent cells.

We acknowledge the support of the Integrated Microscopy Analysis Facility at the University of South Carolina, Heather Muckenfuss, Robert and Margret Salters, and Limin Fu. We also thank Phillip Page of Devro-Teepak for expert technical assistance in the machine design. Digital Instruments and Dr. Irene Revenko are thanked for assistance with the Atomic Force Microscopy on this project.

This work was supported by Devro-Teepak, Dr. Fredric R. Miller, and Dr. Joseph R. Pounder. This work also supported by National Heart, Lung, and Blood Institute Grants HL-58893, HL-42249, and HL-37669.

REFERENCES

1. **Baldwin HS and Buck CA.** Integrins and other cell adhesion molecules in cardiac development. *Trends Cardiovasc Med* 4: 178–187, 1994.
2. **Borg TK, Rubin K, Carver W, Samuel A, and Terracio L.** The cell biology of the cardiac interstitium. *Trends Cardiovasc Med* 6: 65–70, 1996.
3. **Borg TK, Xuehui M, Hilenski L, Vison N, and Terracio L.** The role of the extra cellular matrix on myofibrillogenesis in vitro. In: *Developmental Cardiology: Morphogenesis and Function*, edited by Clark EB and Takano A. Mount Kisco, NY: Futura, 1990, p. 175–189.
4. **Carver Nagpal WML, Nachtigal M, Borg TK, and Terracio L.** Collagen expression in mechanically stimulated cardiac fibroblasts. *Circ Res* 69: 116–122, 1991.
5. **Clark WA, Rudnick SJ, LaPres JJ, Anderson LC, and Lapointe MC.** Regulation of hypertrophy and atrophy in cultured adult heart cells. *Circ Res* 73: 1163–1176, 1993.
6. **Clark WA, Rudnick SJ, LaPres JJ, Lesch M, and Decker RS.** Hypertrophy of isolated adult feline heart cells following β -adrenergic-induced beating. *Am J Physiol Cell Physiol* 261: C530–C542, 1991.
7. **Gordon EE, Kira Y, Demers LM, and Morgan HE.** Aortic pressure as a determinant of cardiac protein degradation. *Am J Physiol Cell Physiol* 250: C932–C938, 1986.
8. **Gordon EE, Kira Y, and Morgan HE.** Aortic perfusion pressure, protein synthesis and protein degradation. *Circulation* 75: 178–180, 1987.
9. **Harris AK.** Cell motility and the problem of anatomical homeostasis. *J Cell Sci Suppl* 8: 121–140, 1987.
10. **Izumo S, Lompre AM, Matsuoka R, Koren G, Schwartz K, Ginard-Nadal B, and Mahdavi V.** Myosin heavy chain messenger RNA and Protein isoform transitions during cardiac hypertrophy. Interaction between hemodynamic and thyroid-induced signals. *J Clin Invest* 79: 977–979, 1987.
11. **Kent RL, Mann DL, and Cooper G.** Signals for cardiac muscle hypertrophy in hypertension. *J Cardiovasc Pharmacol* 17, Suppl 2: S7–S13, 1991.
12. **Klein I, Samarel AM, Welikson R, and Hong C.** Heterotropic cardiac transplantation decreases the capacity for rat myocardial protein synthesis. *Circ Res* 68: 1100–1107, 1991.
13. **Langemyr L, Nordmark A, Ringh M, Ruhe A, Ooppelstrup J, and Dorobantu M.** Partial differential equation toolbox, for use with MATLAB. *MATLAB Manual*. Natick, MA: Mathworks, 1995, p. 2-36–2-42.
14. **Lee AA, Delhaas T, Waldman LK, MacKenna DA, Villarreal FJ, and McCulloch AD.** An equibiaxial strain system for cultured cells. *Am J Physiol Cell Physiol* 271: C1–C9, 1996.
15. **Marieb EN.** *Human Anatomy and Physiology* (2nd ed.). Redwood City, CA: Benjamin/Cummings, 1992, p. 250–253.
16. **Ojamaa K, Petrie JF, Balkman C, Hong C, and Klein I.** Posttranscriptional modification of myosin heavy chain gene expression in the hypertrophied rat myocardium. *Proc Natl Acad Sci USA* 91: 3468–3472, 1994.
17. **Prockop DJ and Guzman NA.** Collagen diseases and the biosynthesis of collagen. *Hosp Pract (Off Ed)* 12: 61–68, 1977.
18. **Raven PH and Johnson GB.** *Biology* (2nd ed.). St. Louis, MO: Times Mirror/Mosby College, 1989, p. 1021–1022.
19. **Rodriguez F.** *Principles of Polymer Systems* (2nd ed.). New York: McGraw-Hill, 1982, Table A. 3.3, p. 315.
20. **Sadoshima J and Izumo S.** Mechanical stretch rapidly activates multiple signal transduction pathways in cardiac myocytes: potential involvement of an autocrine/paracrine mechanism. *EMBO J* 12: 1981–1692, 1993.
21. **Sadoshima J, Jahn L, Takahashi T, Kulik, TJ, and Izumo, S.** Molecular characterization of the stretch-induced adaptation of cultured cardiac cells. An in vitro model of load-induced cardiac hypertrophy. *J Biol Chem* 267: 10551–10560, 1992.
22. **Samarel AM and Englemann GL.** Contractile activity modulates myosin heavy chain- β expression in neonatal rat heart Cells. *Am J Physiol Heart Circ Physiol* 261: H1067–H1077, 1991.
23. **Samarel AM, Spragia ML, Maloney V, Kamal SA, and Englmann GL.** Contractile arrest accelerates myosin heavy chain degradation in neonatal rat heart cells. *Am J Physiol Cell Physiol* 263: C642–C652, 1992.
24. **Simpson DG, Carver W, Borg TK, and Terracio L.** Role of mechanical stimulation in the establishment and maintenance of muscle cell differentiation. *Int Rev Cytol* 150: 69–89, 1994.
25. **Simpson DG, Terracio L, Terracio M, Price RL, Turner DC, and Borg TK.** Modulation of cardiac myocyte phenotype in vitro by the composition and orientation of the extracellular matrix. *J Cell Physiol* 161: 89–105, 1994.
26. **Terracio L, Peters W, Durig B, Miller B, Borg K, and Borg TK.** Cellular hypertrophy can be induced by cyclical stretch in vitro. *Tissue Engin:* 51–56, 1988.
27. **Terracio L and Rubin K.** Expression on collagen binding integrins during cardiac development and hypertrophy. *Circ Res* 68: 734–744, 1991.
28. **Terracio L, Tingstrom A, Peters WH, and Borg TK.** A potential role for mechanical stimulation in cardiac development. *Ann NY Acad Sci* 588: 48–60, 1990.
29. **Vandenburgh HH and P. Karlich.** Longitudinal growth of skeletal myotubes in vitro in a new horizontal mechanical stimulator. *In Vitro* 25: 607–616, 1989.
30. **Xenophontos XP, Gordon EE, and Morgan HE.** Effect of intraventricular pressure on protein synthesis in arrested rat hearts. *Am J Physiol Cell Physiol* 251: C95–C98, 1986.